Active Tactile Object Exploration with Gaussian Processes

Conference Paper · October 2016

DOI: 10.1109/IROS.2016.7759723

7 authors, including:

Roberto Calandra
University of California, Berkeley
14 PUBLICATIONS **62** CITATIONS
SEE PROFILE

Tucker Hermans
University of Utah
16 PUBLICATIONS **99** CITATIONS
SEE PROFILE

Yilei Zhang
Nanyang Technological University
38 PUBLICATIONS **134** CITATIONS
SEE PROFILE

Jan Peters
Technische Universität Darmstadt
340 PUBLICATIONS **6,063** CITATIONS
SEE PROFILE

Active Tactile Object Exploration with Gaussian Processes

Zhengkun Yi[1,2], Roberto Calandra[1], Filipe Veiga[1], Herke van Hoof[1],
Tucker Hermans[3], Yilei Zhang[2], and Jan Peters[1,4]

***Abstract*— Accurate object shape knowledge provides important information for performing stable grasping and dexterous manipulation. When modeling an object using tactile sensors, touching the object surface at a fixed grid of points can be sample inefficient. In this paper, we present an active touch strategy to efficiently reduce the surface geometry uncertainty by leveraging a probabilistic representation of object surface. In particular, we model the object surface using a Gaussian process and use the associated uncertainty information to efficiently determine the next point to explore. We validate the resulting method for tactile object surface modeling using a real robot to reconstruct multiple, complex object surfaces.**

I. Introduction

As robots move from laboratories to domestic environments, they will be required to perform manipulation tasks in unstructured environments. Such robots must be able to achieve sophisticated interactions with the environment and to perform complex tasks such as grasping objects with arbitrary unknown shapes [1], and avoiding slip while applying minimal force to the grasped objects [2]. Object surface property reconstruction plays a vital role in allowing robots to implement these tasks. For instance, shape information is often important for stable grasping as robots can adjust the grasping pose accordingly if shape of the object is known [1]. Surface roughness is closely related to the minimal force applied on the object to counteract slip events [2].

Surface property reconstruction from photos, especially shape reconstruction, has extensively been investigated by the computer vision community [3]–[5]. However, vision-based methods suffer from limitations such as the available illumination and are not applicable when the object is not visible or occluded. In this case, the sense of touch becomes a particularly valuable and complementary sensation to surface property modelling. Compared to vision-based methods, tactile-based approaches are always local [6], i.e., during each touch, only a small part of the object surface can be touched. Thus a robot must touch a given object at several locations along its surface to recover the shape.

State-of-the-art tactile sensors show similar sensing capabilities such as dynamic tactile sensing [7] when compared to humans. In particular, for detecting vibrations, these sensors are more sensitive and accurate than humans [8]. A number of approaches have explored these enhanced capabilities to perform tactile-based object shape reconstruction [6], [9]–[12]. These methods commonly begin with touching the object at a grid of points, which can be sample inefficient for real robot systems. For example, a grid of 50 hand poses is necessary to cover the entire surface of an object when using the Schunk hand in [6]. However, grid search might not be the best solution for object surface reconstruction as adjacent points on the object surface tend to be highly correlated in terms of local geometrical features. In this article, we represent the tactile-based object surface models using Gaussian processes. Based on these models, an active touch strategy is used to reduce the number of sampling iterations necessary for reconstructing the object surface. We demonstrate this approach is capable of achieving faster reconstruction rates when compared to random sampling.

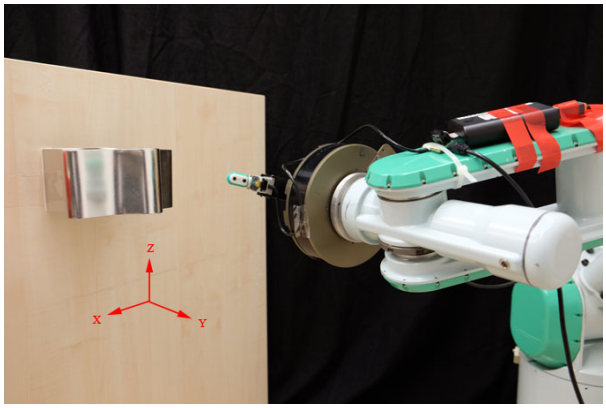

Fig. 1. A BioTac finger mounted on a Mitsubishi PA-10 robot arm equipped with a Schunk force torque sensor. The steel container is fixed to a vertical surface in order to ensure the surface data alignment during each touch. Its front surface is to be reconstructed. The red coordinate frame denotes the axis direction of the world reference frame that is located at the base of the robot.

II. Related Work

Shape is one of the most important surface properties of an object. It can be decomposed into global and local shape [13]. The global shape emphasizes the form of an object, while the local shape is linked to local features such as curvatures and edges.

Montana [9], used the kinematics of contact to estimate the local curvature of an unknown object. The kinematics of contact could be employed in contour following as well under the assumption that the end-effector velocity relative to the immobilized object was measurable by proprioceptive sensors. Jia and Tian [12], presented a method for surface patch reconstruction using "one-dimensional" tactile data.

[1]Intelligent Autonomous Systems Lab, Department of Computer Science, Technische Universität Darmstadt, Hochschulstr. 10, 64289 Darmstadt, Germany {yi, calandra, veiga, hoof, peters}@ias.tu-darmstadt.de

[2]School of Mechanical and Aerospace Engineering, Nanyang Technological University, 50 Nanyang Avenue, Singapore 639798 YIZH0001@e.ntu.edu.sg, ylzhang@ntu.edu.sg

[3]University of Utah Robotics Center, School of Computing, University of Utah, USA thermans@cs.utah.edu

[4]Max Planck Institute for Intelligent Systems, Spemannstr. 38, 72076 Tuebingen, Germany jan.peters@tuebingen.mpg.de

The tactile data was obtained by a two-axis joystick sensor. By simply sliding the fingers over the object surface and using contour tracking techniques, the problem of probing the surface at a grid of points is alleviated. Moll and Erdmann [14], used two tactile sensors to reconstruct an unknown smooth convex planar shape without requiring object immobilization. A closed-form solution regarding the relationship between curvature at the contact points and the rotational speed of the object was provided. Reznik and Lumelsky [15], assumed that every point of the robot hand surface was endowed with the capability of tactile sensing. Based on this assumption, the robot hand was expected to be able to manipulate objects with arbitrary unknown shapes. However, this assumption is quite unrealistic and unfeasible with current technology. Allen and Michelman [11], made an attempt to represent the object surface geometry as a superquadric surface. Dragiev et al. [16], presented a tactile exploration strategy based on Gaussian process implicit shape potential (GPISP) for grasping. The uncertainty aware grasping method improved the performance of tactile exploration. However, this strategy was not implemented on a real robot. Inspired by the method used in mobile robot navigation, Bierbaum et al. [17], presented a tactile exploration strategy with an anthropomorphic five-finger hand. This approach was able to guide the robotic hand along the surface of previously unknown objects.

Traditionally, visual information is prefered for object reconstruction. Li et al. [18], developed a novel tactile sensor known as Gelsight. With this sensor, they were able to reconstruct the 3-D surface geometry of several objects with the aid of photometric stereo algorithms. This new tactile sensing technique was shown to be highly accurate during small parts manipulation and insertion of a USB connector into its socket. Another vision-based tactile sensor was developed to estimate the irregularity of object surfaces [19]. The intensity of the traveling light produced by a LED carries the geometrical information of the touchpad surface. Björkman et al. [10] proposed a probabilistic approach based on Gaussian process regression to enhance visual perception of shape. Tactile measurements iteratively improved the object surface model that was initialized with visual features. Ilonen et al. [20], proposed a method for optimally fusing visual and tactile measurements for symmetrical objects. The visual information was captured by an RGB-D sensor, and tactile information from grasping the unknown object in varying angles was employed to refine the object model.

In this paper, we solely focus on object surface modelling with tactile information. The main contribution is an active touch strategy to reduce the surface geometry uncertainty using a probabilistic representation of the object surface. In particular, we use a Gaussian process in conjunction with the acquisition function to efficiently find the next points to explore.

III. Active Tactile Object Modelling and Exploration

We now focus our attention on our approach for efficiently reconstructing an object surface model. We first describe how to convert our raw tactile measurements into a consistent reference frame. Subsequently, we give a detailed description of estimating an object surface model using a Gaussian process. We then show how we use uncertainty estimates to drive our active tactile data exploration strategy.

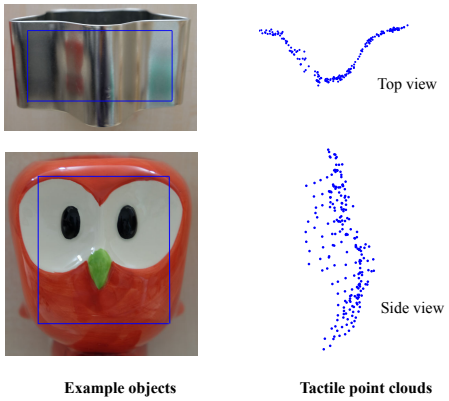

Fig. 2. Example objects (left) and registered tactile point clouds (right) of the front surface of a steel container and the face of a porcelain bird. The rectangular zones are to be reconstructed. The point cloud of the porcelain bird with side view and the point cloud of the front surface of the steel container with top view. Tactile point clouds are obtained with a BioTac tactile sensor.

A. Point Cloud Registration with Tactile Sensing

In our experiments to explore the object surface geometry, the BioTac sensor is used for acquiring the necessary tactile data. The BioTac tactile sensor is a multimodal tactile sensor that pressure, vibration, and temperature [21]. It contains $N_e = 19$ impedance sensing electrodes, which measure the local deformation on the finger surface. We combine these readings into an estimate of a single point of contact (PoC). This estimate is calculated by a weighted average of the Cartesian coordinates of all electrodes. The weights are the impedance values from each of the electrodes. The point of contact (x_c, y_c, z_c) is given by

$$(x_c, y_c, z_c) = \frac{\sum_{i=1}^{N_e} |e_{i^*}|^2 (x_i, y_i, z_i)}{\sum_{i=1}^{N_e} |e_{i^*}|^2}, \qquad (1)$$

where e_{i^*} is the normalized value of the electrodes, and (x_i, y_i, z_i) is the Cartesian coordinate of each electrode on the finger surface. The obtained PoC is in a coordinate frame attached locally to the BioTac. In order to use these PoC estimates for surface reconstruction, we must transform the position $\mathbf{m}_n = (x_c, y_c, z_c)$ into the our world coordinate frame using the robot's forward kinematics. We denote the transformed point $\mathbf{x}_n$. Fig. 2 depicts the two objects we used in experiments along with registered point clouds built from tactile data samples.

B. Gaussian Processes as Surface Models

Gaussian processes (GPs) [22] are a powerful tool for regression problems. In this paper, we use Gaussian processes to model object surfaces. These models are a probabilistic representation of the surface geometry. While implicit surface models have been proposed using GPs [10], [23], we elect to use an explicit representation in order to avoid

the need of creating artificial interior and exterior boundary points to stabilize the surface model. However, the active touch approach we present is still valid for the implicit GP model, as long as some care is taken to account for these artificial points. Our explicit model of the surface takes the form $y_n = f(x_n, z_n)$, with (x_n, y_n, z_n) defined as the contact coordinate, $\mathbf{x}_n$, in the world reference frame (refer to Fig. 1).[1]

A GP is fully specified by mean function $\mu(\tilde{\mathbf{x}})$ and covariance function $k(\tilde{\mathbf{x}}_i, \tilde{\mathbf{x}}_j)$. Where $\tilde{\mathbf{x}}_i = (x_i, z_i)$. We choose as covariance function the squared exponential

$$k(\tilde{\mathbf{x}}_i, \tilde{\mathbf{x}}_j) = \sigma_f^2 \mathrm{e}^{-\frac{1}{2}(\tilde{\mathbf{x}}_i - \tilde{\mathbf{x}}_j)^T \mathbf{\Lambda}^{-1} (\tilde{\mathbf{x}}_i - \tilde{\mathbf{x}}_j)} + \sigma_w^2 \delta_{ij}, \quad (2)$$

where $\mathbf{\Lambda}$ is a diagonal matrix and δ_{ij} is the Kronecker delta. The prior mean function $\mu(\tilde{\mathbf{x}})$ is specified by $\mu(\tilde{\mathbf{x}}) = 0$. We define the training data set as $\mathbf{T} = [(\tilde{\mathbf{x}}_1, y_1), \ldots, (\tilde{\mathbf{x}}_N, y_N)]$. For a new observation $\tilde{\mathbf{x}}_*$, the predictive distribution of a GP is Gaussian with the mean $\mu(\tilde{\mathbf{x}}_*)$ and the variance $\sigma^2(\tilde{\mathbf{x}}_*)$

$$\mu(\tilde{\mathbf{x}}_*) = \mathbf{k}_*^T \mathbf{K}^{-1} \mathbf{y}, \;\; \sigma^2(\tilde{\mathbf{x}}_*) = k_{**} - \mathbf{k}_*^T \mathbf{K}^{-1} \mathbf{k}_*, \quad (3)$$

where $\mathbf{k}_*$ is a vector with N entries $k(\tilde{\mathbf{x}}_i, \tilde{\mathbf{x}}_*)$, $\mathbf{K}$ is the matrix with $\mathbf{K}_{ij} = k(\tilde{\mathbf{x}}_i, \tilde{\mathbf{x}}_j)$ and $k_{**} = k(\tilde{\mathbf{x}}_*, \tilde{\mathbf{x}}_*)$. The posterior mean defines an estimate of the object's shape and the posterior variance defines the uncertainty regarding the unexplored area.

C. Action Selection

Due to the inherent locality of tactile sensing, a robot must touch an object at multiple locations in order to cover the entire surface of the object. Performing many touch actions can be sample inefficient. We devise an efficient strategy for deciding the next touch action in order to reduce the total number of object probes. By updating the probabilistic representation given in Equation 3 after each touch, we can employ a straightforward strategy for exploring the object.

We draw our inspiration from Bayesian optimization (BO), which uses different "acquisition functions" to address the choice of which point to sample from a target object function when performing black-box optimization in an iterative manner [24]. BO has been used in various robotic applications such as gait optimization [25], grasp optimization [26], and policy search [27]. In the literature, a number of acquisition functions $\alpha(\tilde{\mathbf{x}})$ have been proposed, such as upper confidence bound (UCB) [28], probability of improvement (PI) [29] and expected improvement (EI) [30]. All of these proposed acquisition functions implicitly handle the exploration versus exploitation trade-off. Our active touch approach focuses on exploration of uncertain surface regions and thus does not need to account for exploitation of well-known surface areas. We base our acquisition function on the predicted standard deviation, $\sigma(\tilde{\mathbf{x}})$, as it can be seen as a measures of surface uncertainty at a given location. The surface point with highest uncertainty serves as a good candidate for the next touch location, as it is either far from any recorded measurements or near areas of large surface variation. We thus define our acquisition function as $\alpha(\tilde{\mathbf{x}}) = \sigma(\tilde{\mathbf{x}})$. Our active tactile exploration approach is outlined in Algorithm 1, and it will be subsequently referred to as the "active touch method". To find the global optima of the acquisition function, we use DIRECT [31] to find the approximately optimal solution, which is subsequently refined by LBFGS [32].

[1]The choice of predicting the y-component instead of x or z is arbitrary. We have selected y as it was the direction the robot arm moves in our experimental setup.

Algorithm 1 Active Tactile Exploration with GPs

Initialize:

Store N initial points $\mathbf{T} = [(\tilde{\mathbf{x}}_1, y_1), \ldots, (\tilde{\mathbf{x}}_N, y_N)]$.

Loop:

1) Train a GP surface model based on $\mathbf{T}$.
2) Calculate acquisition function,
$$\alpha(\tilde{\mathbf{x}}) = \sigma(\tilde{\mathbf{x}}).$$
3) Find the optimal value $\tilde{\mathbf{x}}^*$ of $\alpha(\tilde{\mathbf{x}})$,
$$\tilde{\mathbf{x}}^* = \arg\max_{\tilde{\mathbf{x}}} \alpha(\tilde{\mathbf{x}}).$$
4) Evaluate $\tilde{\mathbf{x}}^*$ and obtain y^* from the robot.
5) Add $(\tilde{\mathbf{x}}^*, y^*)$ to data set $\mathbf{T}$.

IV. Experiments and Results

We evaluate our active touch method on a benchmark task and realistic experiments. First, we validate the proposed method on a 1-D toy example. Second, we apply the active tactile exploration approach to the task of object surface reconstruction using a real robot. As a baseline, we compare to a method which chooses touch locations uniformly randomly.

A. Proof of Concept: A Toy Example

The toy example is a 1-D function which consists of a curved part and a flat part. It is defined as

$$f(x) = \begin{cases} \sin(\omega x) + 1 & \text{if } -1 \leq x \leq 1 \\ 1 & \text{if } -2 \leq x < -1 \text{ or } 1 < x \leq 2, \end{cases} \quad (4)$$

where $\omega = 4\pi$.

The active exploration process for an unknown 1-D function is illustrated in Fig. 3. The top and bottom row represent the optimization process with the random and active touch approaches respectively. The green curve shows the true function. The shaded area (red and blue) represents the 95% confidence bound of the GP model. The exploration process is initialized with five random points (shown as blue crosses). These points are also used to initialize the GP models. The maximum of the acquisition function determines the next points (i.e. the red crosses) to be explored by the active exploration method. The GP models are updated after each sampling iteration. After a few iterations, the GPs could accurately model the true function. We conclude that the active touch method is more accurate at reconstructing the unknown 1-D curve while using fewer points than the random touch method. In this experiment, we quantify the similarity between the true function and the reconstructed function by measuring the correlation coefficient between

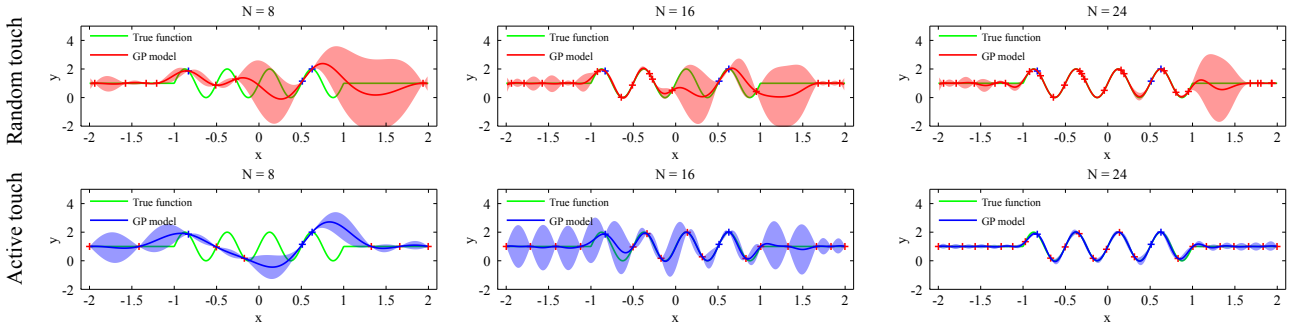

(a) 8 evaluations (b) 16 evaluations (c) 24 evaluations

Fig. 3. A toy example of the active exploration process for reconstructing an unknown 1-D surface (green curve). The 95% confidence of the model prediction is represented by the shaded area. The red (top) and blue area (bottom) represent optimization based on random touch, and on active touch respectively. The surface model is initialized with 3 random points (blue crosses). The subsequent points to explore are marked with red crosses. At each iteration, the model is updated using all the obtained points (both blue and red crosses). After a few iterations, the active touch method is able to reconstruct the unknown 1-D curve more accurately.

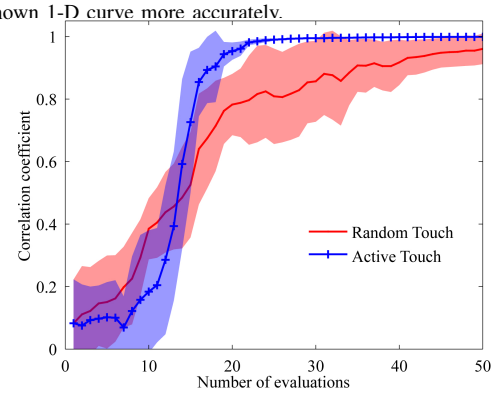

Fig. 4. The correlation coefficient over 50 evaluations for both the random and active touch. Both methods are initialized with 3 random touches. The shaded areas represent the standard error. The correlation coefficient between the real function and reconstructed function almost reaches 1 after 23 touches with the active touch approach.

the two, defined by:

$$R = \frac{\int f(x)\hat{f}(x)dx}{\sqrt{\int f(x)^2 dx \int \hat{f}(x)^2 dx}}, \tag{5}$$

where $f(x)$ and $\hat{f}(x)$ are the true function and reconstructed function respectively. The integrals in Equation 5 are approximated as sums over the test set. Fig. 4 shows the average correlation coefficient between the real and predicted function over ten trials for both the active and the random touch method. As expected, the correlation coefficient almost converges to 1 much faster when using the active touch approach. The random approach obtains a higher correlation coefficient initially up until about 15 samples. We attribute this to the hyperparemeter estimation being overly-confident, causing the system to select a larger characteristic length-scale than the true function. We could potentially fix this by bounding the length scale to some maximum value, proportional to the desired resolution of our result. We leave this to future work.

B. Tactile Object Surface Modelling

We explain how we perform tactile object surface modeling using a real robot. Starting with a description of the experimental robot platform, we follow with a detailed explanation of the tactile data collection procedure. Finally, we present the results of the tactile object surface reconstruction.

Experimental Setup: The experiments were conducted on a Mitsubishi PA-10, a robot arm with seven degrees of freedom. A BioTac tactile sensor, used to touch the object, is rigidly attached to a force-torque sensor. The force-torque sensor is mounted to the end effector of the robot arm. It allows the robot to perceive the force exerted on the object, and is used in order to avoid any unexpected collisions. An inverse Jacobian controller is implemented to drive the robot end effector to the desired task space locations. The objects used include the steel container and porcelain bird shown in Figure 2. We affix the objects to a vertical surface in order to ensure that the surface data remains aligned during the entire data collection procedure. The complete setup can be seen in Fig. 1. In addition to the signals from 19 electrical impedance electrodes, the BioTac sensor produces another four types of tactile signals: absolute fluid pressure (PDC) signal, dynamic fluid vibration (PAC) signal, temperature (TDC) and heat flow (TAC). In our experiments, a contact between the BioTac finger and touched objects is considered to occur if a change in the absolute fluid pressure passes a small threshold.

Data Collection: The area to be reconstructed for both the steel container and the porcelain bird is constrained to a predefined rectangular zone (refer to Fig. 2). For both the random and active touch approaches, the first several touches are randomly performed. Specifically, a random value of (x, z) in the world reference frame is uniformly sampled from the predefined zone, and then the end effector moves in the negative y-axis direction until it detects contact and stops. The actual contact position between the BioTac finger and the object surface is computed using the 19 electrodes and is registered after the homogeneous transformation described in Section III-A. After obtaining these random tactile surface samples, the end effector will move back concluding the random sampling phase. It is worth mentioning that the contact position computed from the BioTac may not have the same (x, z) components as the point chosen by the acquisition functions. This can easily occur since the BioTac will likely make contact with the object at some location other than the commanded position for the finger center.

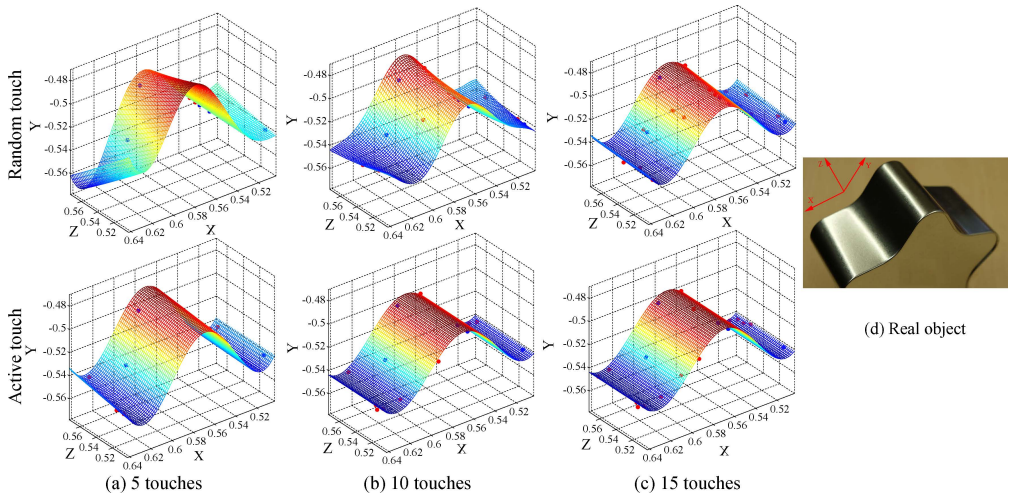

Fig. 5. Evolution of the steel container model as function of the number of touches. The optimization is initialized with 5 random touches (blue points). The subsequent points to explore are marked with red points. The top row represents the model build from random samples. The bottom row shows results for the active touch method. The columns from left to right represent the models after (a) 5, (b) 10, and (c) 15 additional touches. (d) The real object for comparison. Each predicted surface is the mean of the GP computer over the test set. The active touch method more accurately reconstructs the object surface for a given number of samples compared to the random touch approach.

These initial samples are used to initialize the Gaussian process surface model. Subsequent touch locations (x, z) are calculated differently for the active touch and random touch approaches. The active touch approach is based on Algorithm 1, while the random touch approach continues to randomly sample from the predefined zone. The GP model is updated after each sampling iteration. This iterative sampling procedure is repeated by both approaches until a reasonable tactile data set is collected.

Surface Estimation Results: The active exploration process for the steel container is illustrated in Fig. 5. The top and bottom row represent the optimization process of random touch and active touch respectively. The exploration process is initialized with five random touch points (i.e. the blue points). The GP models are initially trained on those random touches and iteratively determine subsequent touch points (i.e. the red points) to explore. The predicted surfaces are the means of GPs computed over the test set. It is shown that the GP models based on active touch accurately model the surface using only ten additional touches. Fig. 6 illustrates an example of using the active touch method to determine the next touch location. We see that the GP models a larger characteristic length-scale of the covariance function in the $Z-$dimension compared to the $X-$dimension. This characteristic was automatically learned by the GP and is consistent with the real object.

Fig. 7 depicts the active exploration process for the porcelain bird. The top and bottom rows represent the exploration strategies of random touch and active touch respectively. Each exploration process is initialized with 20 random touch points (i.e. the blue points). The figure represents the models after 100 additional touches. The active touch method better reconstructs the face of the porcelain bird. In particular, it more accurately models the boundaries of the reconstruction zone. However, both methods fail to model the nose of the porcelain bird. Several factors lead to this issue. First it may be caused either by the smoothness limitations imposed by the covariance function or samples being averaged out in computing the maximum a posteriori (MAP) estimate. This problem arises from data being difficult to collect near the edge of the nose, because of the relatively large size of the BioTac sensor compared to the nose.

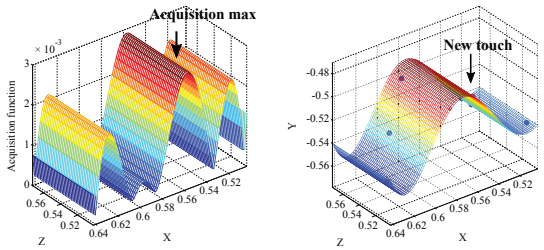

Fig. 6. An example of the active touch method for determining a new touch location. The acquisition function is high where the Gaussian process predicts a high uncertainty (left). The position with the maximum acquisition function value defines the next touch location (right).

V. Conclusions

Tactile object surface reconstruction is a complex task. In this paper, we circumvent exhaustively touching the object in a grid by presenting an active exploration approach. We validate our method on a toy example and on tactile object surface modeling using a real robot. The toy example successfully shows that our active touch approach can reconstruct an unknown 1-D surface more accurately while using fewer points compared to the random touch method. For the tactile object modeling task, our robot strategically chooses the point to be touched. This approach makes a reasonable estimate of an object's shape, while dramatically reducing the exploration time. The reconstructed object features have great promise for a number of applications, such as object recognition and stable grasping. A limiting assumption of our method is, that the object has to be rigid and must be immobilized during the entire data collection procedure.

The presented work can be extended in several directions. We will further incorporate visual perception to facilitate the surface reconstruction. Another interesting direction involves incorporating active contour following, a natural form of exploration used by human beings. Finally, we would like to

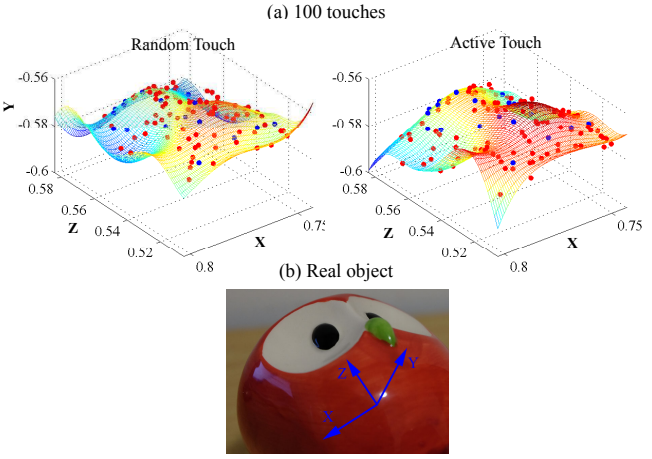

Fig. 7. (a) The porcelain bird models for both the random and active touch approaches with 20 randomly selected initial touches (blue points) and 100 additional touches (red points). (b) The real object for comparison. The predicted surfaces are the means of GPs over the test set. After 100 touches, the active method could model the bird face more accurately, particularly at the edge of the explored zone.

combine the shape information provided by reconstruction with our previous work [33] on tactile object recognition.

VI. Acknowledgments

The research leading to these results has received funding from the European Community's Seventh Framework Programme (FP7/20072013) under grant agreement 610967 (TACMAN). This project is supported by the Joint PhD Degree Programme NTU-TU Darmstadt. The project is also supported by Fraunhofer Singapore, which is funded by the National Research Foundation (NRF) and managed through the multi-agency Interactive & Digital Media Programme Office (IDMPO) hosted by the Media Development Authority of Singapore (MDA). Y.Z. acknowledges financial support from the A*STAR Industrial Robotics Programme (1225100007) and the AOP programme (1223600005).

References

[1] H. Yousef, M. Boukallel, and K. Althoefer, "Tactile sensing for dexterous in-hand manipulation in robotics: A review," *Sensors and Actuators A: Physical*, vol. 167, no. 2, pp. 171–187, 2011.

[2] C. Melchiorri, "Slip detection and control using tactile and force sensors," *IEEE/ASME Transactions on Mechatronics*, vol. 5, no. 3, pp. 235–243, 2000.

[3] S. M. Seitz, B. Curless, J. Diebel, D. Scharstein, and R. Szeliski, "A comparison and evaluation of multi-view stereo reconstruction algorithms," in *IEEE Conference On Computer Vision and Pattern Recognition*, vol. 1, 2006, pp. 519–528.

[4] R. M. Bolle and B. C. Vemuri, "On three-dimensional surface reconstruction methods," *IEEE Transactions on Pattern Analysis and Machine Intelligence*, no. 1, pp. 1–13, 1991.

[5] V. Lippiello, F. Ruggiero, B. Siciliano, and L. Villani, "Visual grasp planning for unknown objects using a multifingered robotic hand," *IEEE/ASME Transactions on Mechatronics*, vol. 18, no. 3, pp. 1050–1059, 2013.

[6] M. Meier, M. Schopfer, R. Haschke, and H. Ritter, "A probabilistic approach to tactile shape reconstruction," *IEEE Transactions on Robotics*, vol. 27, no. 3, pp. 630–635, 2011.

[7] R. D. Howe and M. R. Cutkosky, "Dynamic tactile sensing: Perception of fine surface features with stress rate sensing," *IEEE transactions on robotics and automation*, vol. 9, no. 2, pp. 140–151, 1993.

[8] J. A. Fishel and G. E. Loeb, "Sensing tactile microvibrations with the BioTac - comparison with human sensitivity," in *IEEE/EMBS International Conference on Biomedical Robotics and Biomechatronics*, 2012, pp. 1122–1127.

[9] D. J. Montana, "The kinematics of contact and grasp," *The International Journal of Robotics Research*, vol. 7, no. 3, pp. 17–32, 1988.

[10] M. Björkman, Y. Bekiroglu, V. Högman, and D. Kragic, "Enhancing visual perception of shape through tactile glances," in *IEEE/RSJ International Conference on Intelligent Robotics and Systems*, 2013, pp. 3180–3186.

[11] P. K. Allen and P. Michelman, "Acquisition and interpretation of 3-D sensor data from touch," in *Interpretation of 3D Scenes, 1989. Proceedings., Workshop on*. IEEE, 1989, pp. 33–40.

[12] Y.-B. Jia and J. Tian, "Surface patch reconstruction from "one-dimensional" tactile data," *Automation Science and Engineering, IEEE Transactions on*, vol. 7, no. 2, pp. 400–407, 2010.

[13] S. Salehi, J.-J. Cabibihan, and S. S. Ge, "Artificial skin ridges enhance local tactile shape discrimination," *Sensors*, vol. 11, no. 9, pp. 8626–8642, 2011.

[14] M. Moll and M. A. Erdmann, "Reconstructing shape from motion using tactile sensors," *Robotics Institute*, p. 239, 2001.

[15] D. Reznik and V. Lumelsky, "Multi-finger "hugging": a robust approach to sensor-based grasp planning," in *IEEE International Conference on Robotics and Automation*, 1994, pp. 754–759.

[16] S. Dragiev, M. Toussaint, and M. Gienger, "Uncertainty aware grasping and tactile exploration," in *IEEE International Conference on Robotics and Automation*, 2013, pp. 113–119.

[17] A. Bierbaum, M. Rambow, T. Asfour, and R. Dillmann, "A potential field approach to dexterous tactile exploration of unknown objects," in *IEEE/RAS International Conference on Humanoid Robots*, 2008, pp. 360–366.

[18] R. Li, R. Platt, W. Yuan, A. ten Pas, N. Roscup, M. A. Srinivasan, and E. Adelson, "Localization and manipulation of small parts using Gelsight tactile sensing," in *IEEE/RSJ International Conference on Intelligent Robotics and Systems*, 2014, pp. 3988–3993.

[19] Y. Ito, Y. Kim, C. Nagai, and G. Obinata, "Vision-based tactile sensing and shape estimation using a fluid-type touchpad," *Automation Science and Engineering, IEEE Transactions on*, vol. 9, no. 4, pp. 734–744, 2012.

[20] J. Ilonen, J. Bohg, and V. Kyrki, "Fusing visual and tactile sensing for 3-d object reconstruction while grasping," in *IEEE International Conference on Robotics and Automation*, 2013, pp. 3547–3554.

[21] N. Wettels, J. A. Fishel, and G. E. Loeb, "Multimodal tactile sensor," in *The Human Hand as an Inspiration for Robot Hand Development*. Springer, 2014, pp. 405–429.

[22] C. E. Rasmussen, *Gaussian Processes for Machine Learning*. The MIT Press, 2006.

[23] S. Dragiev, M. Toussaint, and M. Gienger, "Gaussian process implicit surfaces for shape estimation and grasping," in *IEEE International Conference on Robotics and Automation*, 2011, pp. 2845–2850.

[24] J. Snoek, H. Larochelle, and R. P. Adams, "Practical Bayesian optimization of machine learning algorithms," in *Advances in neural information processing systems*, 2012, pp. 2951–2959.

[25] R. Calandra, A. Seyfarth, J. Peters, and M. P. Deisenroth, "Bayesian optimization for learning gaits under uncertainty," *Annals of Mathematics and Artificial Intelligence (AMAI)*, vol. 76, no. 1, pp. 5–23, 2015.

[26] A. Boularias, J. A. Bagnell, and A. Stentz, "Efficient optimization for autonomous robotic manipulation of natural objects," in *The Twenty-Eighth AAAI Conference on Artificial Intelligence*, 2014, pp. 2520–2526.

[27] R. Martinez-Cantin, N. de Freitas, A. Doucet, and J. A. Castellanos, "Active policy learning for robot planning and exploration under uncertainty," in *Robotics: Science and Systems*, 2007, pp. 321–328.

[28] D. D. Cox and S. John, "SDO: A statistical method for global optimization," *Multidisciplinary design optimization: state of the art*, pp. 315–329, 1997.

[29] H. J. Kushner, "A new method of locating the maximum point of an arbitrary multipeak curve in the presence of noise," *Journal of Basic Engineering*, vol. 86, no. 1, pp. 97–106, 1964.

[30] J. Mockus, V. Tiesis, and A. Zilinskas, "The application of bayesian methods for seeking the extremum," *Towards global optimization*, vol. 2, no. 117-129, p. 2, 1978.

[31] D. R. Jones, C. D. Perttunen, and B. E. Stuckman, "Lipschitzian optimization without the Lipschitz constant," *Journal of Optimization Theory and Applications*, vol. 79, no. 1, pp. 157–181, 1993.

[32] R. H. Byrd, P. Lu, J. Nocedal, and C. Zhu, "A limited memory algorithm for bound constrained optimization," *SIAM Journal on Scientific Computing*, vol. 16, no. 5, pp. 1190–1208, 1995.

[33] J. Hoelscher, J. Peters, and T. Hermans, "Evaluation of tactile feature extraction for interactive object recognition," in *IEEE/RAS International Conference on Humanoid Robots*, 2015.